

Distribution of Solar Irradiance on Inclined Surfaces Due to the Plane of the Ground

Teolan Tomson^{1*}, Henrik Voll²

¹Institute of Materials Science, Tallinn University of Technology (TUT), Tallinn, Estonia

²Department of Environmental Engineering, Tallinn University of Technology (TUT), Tallinn, Estonia

Email: teolan62@gmail.com

Received 15 May 2014; revised 18 June 2014; accepted 27 June 2014

Copyright © 2014 by authors and Scientific Research Publishing Inc.

This work is licensed under the Creative Commons Attribution International License (CC BY).

<http://creativecommons.org/licenses/by/4.0/>



Open Access

Abstract

Measurements of solar radiation are ordinarily made on horizontal planes recording global, diffuse and reflected components. The beam component and distribution of the global radiation on tilted planes can be calculated via the said components, as the position of the Sun in the sky's sphere is known. Another ordinary procedure is measuring beam and diffuse components and calculating global radiation. These measurements require stationary equipment and in such a way it is difficult to study the influence of different grounds on the distribution of radiation on the inclined surfaces due to the ground. This distribution has some importance in civil engineering, but it is not popular in the field of solar radiation investigations. Present paper shows how this distribution can be calculated measuring only global irradiance on the horizontal and vertical planes. Such an approach, which is valid in clear-sky and overcast conditions, allows the use of a portable measuring device and studies of different grounds. The coincidence of the calculated values with the actual is good, except for snow-cover and discrete cloud, which do not correspond to the isotropic sky and ground models.

Keywords

Solar Irradiance, Hanging Down Façade, Ground Influence

1. Introduction

In order to achieve the nearly zero energy building (nZEB) requirements by 2021, energy efficient façades are one important factor in the design of such buildings [1]. Passive architectural cooling and heating have a strong impact on the heating, cooling and electric lighting energy needs, as well as on daylight.

*Corresponding author.

A self-shading façade that is an inclined surface, due to the plane of the ground, is one option among passive cooling strategies. **Figure 1** and **Figure 2** show such buildings in Tallinn, Estonia. The role of alternative passive design principals in nZEB buildings is a well-studied topic. However, self-shading façades have garnered very little attention [2]. The distribution of solar irradiance on inclined surfaces, due to the plane of the ground, has been theoretically studied in connection with reflected radiation [3]-[5].

The manner in which irradiance is distributed on walls with a hanging façade, essentially influenced by reflected radiation, should be of interest. The experimental study of the actual distribution supports the expected theoretical model, which is the goal of this study. The theoretical model corresponds to the isotropic sky, which exists in clear-skies and overcast conditions. Under conditions of discrete alternating clouds, the distribution law differs [6], but it is not discussed in the present study.

2. Theoretical Background

Although solar energy is carried by global radiation, it is expedient to handle it according to its components: beam, diffuse and reflected radiation. It is also expedient to consider including circumsolar diffuse radiation as part of beam radiation, as typical flat-plate solar collectors and walls do not differentiate between them.

In the current research horizontal brightening is assumed to be negligible due to its small share (in an urban environment). In **Figure 3** the components of radiation considered in the theoretical model are described, which is created in the vertical plane along the Sun's current azimuth Φ . G_0 is the measured value of irradiance picked up by the horizontal sensor S(0). G_{FV} is the measured value of irradiance picked up by the vertical sensor S(90) at the azimuth " Φ " (turned directly into the Sun). G_{BV} is the measured value of irradiance picked up by the vertical sensor S(-90) at the azimuth " $\Phi + 180$ " (turned away from the Sun). G_r is the measured value of irradiance picked up by the backward horizontal sensor S(180)—recording the pure reflected radiation. All these values are known by measurements and can be used as inputs in the calculation. Sensors S(-90) and S(180) are always located in shadow, which means that the beam component is lacking in G_{BV} and G_r . Correspondingly, in the isotropic sky model [7] and isotropic ground model [3] the sum of diffuse and reflected radiation exists on all planes, equally on the illuminated or shadowed side of the carrier ring, where the sensors S(0) - S(180) are installed.

Additionally, the beam component exists on the illuminated sector only¹ and its value depends on the beam radiation G_b and attack angle Θ_T . building the model in the plane of the Sun's azimuth, a simple relation is valid $\Theta_T = \pi/2 - \alpha_s - \beta$. This knowledge allows a flow diagram of the theoretical calculations to be composed [8], see **Figure 4**, where the known variables are the tilt angle β and the Sun's height angle α_s . The flow diagram and text uses values relative to G_0 , marked with an asterisk

$$G^* = G/G_0 . \quad (1)$$

When creating the flow diagram, the fact is used that sensor S(-90) is always in shadow, and the sum of the isotropic diffuse and reflected radiation can be expressed as

$$G_{BV}^* = G_r^* \cdot (1 - \cos \beta) / 2 + G_{d0}^* \cdot (1 + \cos \beta) / 2 . \quad (2)$$

Considering that at $\beta = -90^\circ$ its cosine is zero, $\cos \beta = 0$, it results $G_{d0}^* = 2 \cdot G_{BV}^* - \mathcal{A}$, where \mathcal{A} is the albedo. This theoretical model is compared below with actual (measured) relative values of irradiance on the inclined planes in different conditions and on different types of surfaces.

3. Hardware for the Measurements

In order to measure the irradiance on inclined surfaces due to the plane of the ground, a special portable stand was constructed. The stand has a carrier ring with six sensors and a frame, see **Figure 5**. Sensor S(0) measures global radiation on the horizontal plane G_0 , sensor S(90) measures the same on the vertical plane G_V , and sensor S(180) measures pure reflected radiation G_r . Sensors S(112.5), S(135) and S(157.5) measure radiation on corresponding planes. The whole stand can be turned directly into the Sun's azimuth Φ , or away from it, or to any free azimuth $\Phi \pm \gamma$; $\gamma \in \{30, 60 \dots 180\}$. The sensors used were Danish-made photoelectrical pyranometers [9], which have a transient time of microseconds and allow for the dynamic behavior of (reflected) radiation to be studied.

¹Of course, if the sun is shining.

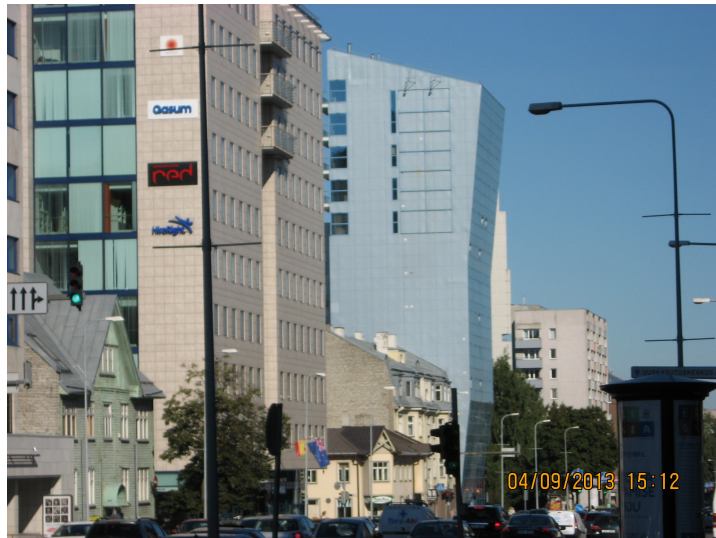


Figure 1. A self-shaded façade in Tallinn Estonia (Liivalaia Street).



Figure 2. A self-shaded façade in Tallinn Estonia (St. Petersburg Highway).

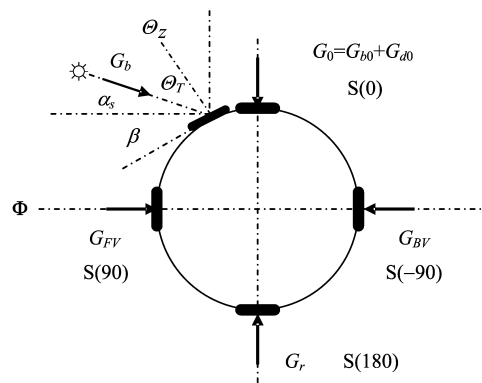


Figure 3. Components of radiation, which are used in theoretical calculations.

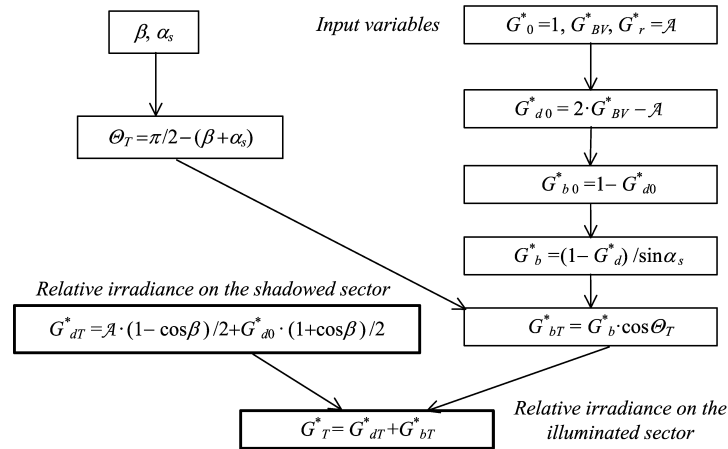


Figure 4. Flow diagram for the theoretical calculations of relative irradiance on tilted planes.

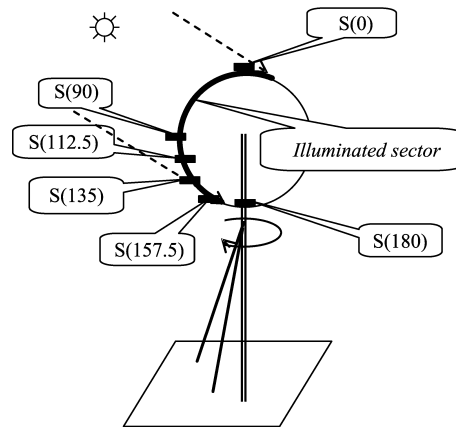


Figure 5. Portable stand for measurements.

The height of sensor S(180) is 1.85 m above the ground (1.5 m above the water). Under sunny conditions, a sector (180°) of the carrier ring is always illuminated by beam radiation, although the position of this illuminated sector depends on the height angle of the Sun α_s . The said ring is transported separately and in each measuring session connected to the frame.

The frame has an aluminum vertical post for the carrier ring and two supporting legs under ~30° angles. The vertical position of the post can be controlled by a plumb line and rotated around 360°. In this way, all required azimuths could be controlled.

On weak surfaces: rank grass, thick snow and the (slippery and tilted) bottom of a pond, the operator has to support the frame. The influence of the stand on the accuracy of the measurements is discussed below. Therefore, the accuracy of the vertical position can be evaluated in the range $\pm 5^\circ$. The entire structure of the frame has been painted black, to avoid any possible reflections. The influence of the stand on the accuracy of the measurements is discussed below. **Figure 6** shows the complex measurement device for measurements on a limestone gravel surface. Other tested surfaces were snow (fresh and old), asphalt, sand, grass (rank and sparse) and water (still).

4. Methodical Introduction

Measured global irradiance was recorded using a midilogger 200 data logger and the results presented below are the average values of 20 - 30 s recordings in relative units $G_T^* = G_T / G_0$, where G_T is irradiance on the tilted plane and G_0 is irradiance on the horizontal plane. The first measurements were taken while turned directly into the Sun's azimuth "Φ" and then the stand was turned clockwise to the next position. Azimuth increments of 30° were used, and during simplified measurements this increment was 90°. Measurements were taken in clear-sky



Figure 6. Measurements of radiation on a limestone gravel surface.

or in overcast conditions. In some cases, a visor was used to protect S(90) from beam radiation; these measurements will be highlighted with an additional comment. **Figure 7** shows the distribution of relative irradiance in clear-sky conditions, on the ground (a cultivated landfill-hill of Tallinn, 59.36°N, 24.65°E, 60 m a.s.l.) covered by rank grass, depending on the azimuth and tilt angle.

Due to the practically coinciding lines of the sensors S(135) - S(180) these are united and marked in **Figure 7** as “<135”. The diagram in **Figure 8** was recorded in a car park with an asphalt surface and it shows the distribution of relative irradiance in overcast conditions, depending on the azimuth and tilt angle.

The diagram in **Figure 8** was recorded at the stadium of Tallinn Technical University, which is covered with sparse grass. Dotted grid lines in **Figure 7** and **Figure 8** mark values 1.2 and 0.6, respectively. The theory of the distribution of irradiance and similar measurements in conditions of discrete alternating cloud requires a special study and is beyond the scope of this paper.

5. Results and Discussion

Comparisons of the calculated and measured values of irradiance under different conditions using relative values are presented in this section. The lines in the following figures mean the following: G_{dT}^* —calculated diffuse irradiance on tilted planes; G_{rT}^* —calculated reflected irradiance on tilted planes; G_{bT}^* —calculated beam irradiance on tilted planes; G_T^* —calculated global irradiance on tilted planes; G_a^* —measured actual irradiance on tilted planes. For each diagram, recording data and a short comment are added.

The coincidence of G_T^* and G_a^* is good in the shadowed and almost satisfactory in the illuminated sectors (see **Figure 9**). These measurements were taken on the hill of the closed and cultivated Tallinn landfill, with an absolute unobstructed horizon.

The coincidence of G_T^* and G_a^* is not quite satisfactory due to the Sun being hidden and satisfactory away from the Sun (see **Figure 10**). These measurements were taken in the stadium of Tallinn University of Technology, surrounded by low forest (height of the optical barrier is ~15°), and possibly influenced by the (nearest ~70 m) forest.

The coincidence of G_T^* and G_a^* is good (see **Figure 11**) both in the shadowed and the illuminated sectors. These measurements were taken in the car park of a shopping center.

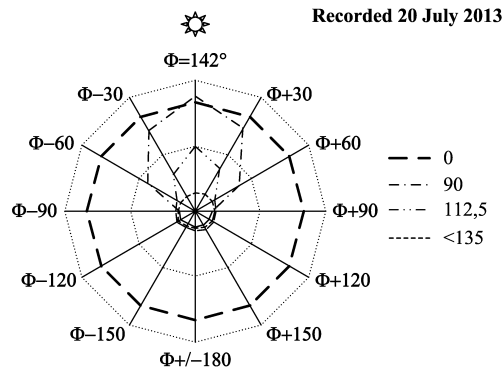


Figure 7. Dependence of irradiance on azimuth Φ and tilt angle $\beta \in \{90^\circ - 180^\circ\}$ in sunshine.

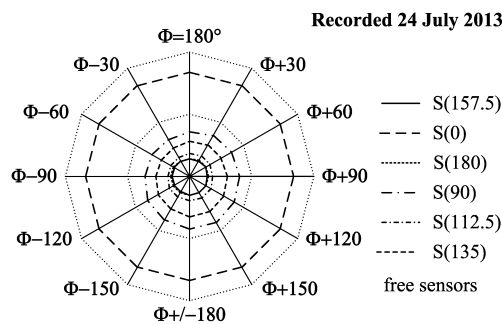


Figure 8. Dependence of irradiance on azimuth Φ and tilt angle $\beta \in \{90^\circ - 180^\circ\}$ in shadow.

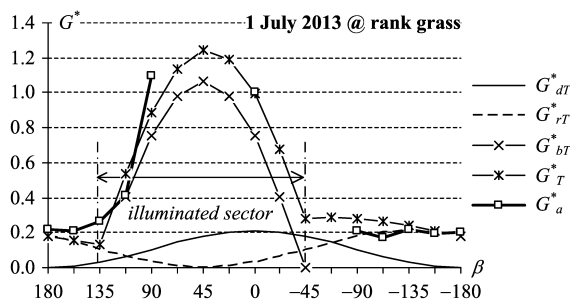


Figure 9. Rank grass in sunshine: $G_0 = 793 \text{ Wm}^{-2}$; $\alpha_s = 44.8^\circ$ and $\mathcal{A} = 0.21$.

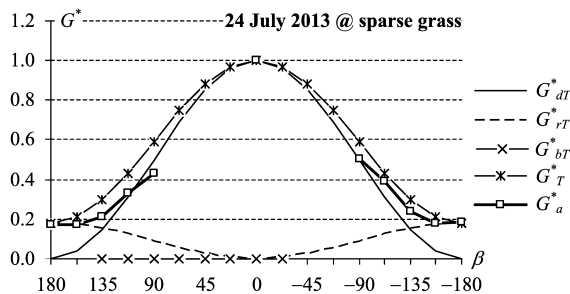


Figure 10. Sparse grass under an overcast sky (in shadow): $G_0 = 187 \text{ Wm}^{-2}$; $\alpha_s = 39.4^\circ$ and $\mathcal{A} = 0.18$.

The coincidence of G_T^* and G_a^* is not quite satisfactory (see **Figure 12**), due to the Sun being hidden, and satisfactory away from the Sun. Possibly the result is distorted due to several large trucks being parked at a distance of ~50 m.

The coincidence of G_T^* and G_a^* is good in the shadowed and not quite as satisfactory in the illuminated sectors (see **Figure 13**).

The coincidence of G_T^* and G_a^* is good in both the shadowed and the illuminated sectors (see **Figure 14**).

In this experiment, S(90) was covered with an upper visor which blocked beam radiation.

It is shown that irradiance in the vertical plane @S(90) is now less than the pure reflected irradiance measured with S(180), which coincides with the theoretical model. The coincidence of G_T^* and G_a^* is good in both the shadowed and the illuminated sectors (see **Figure 15**).

The coincidence of G_T^* and G_a^* is very good in both the shadowed and the illuminated sectors (see **Figure 16**).

The coincidence of G_T^* and G_a^* is very good in the shadowed sector (see **Figure 17**), but it is principally different in the illuminated sector. It is not a failure: this experiment was repeated three times and in different locations; however, the results were always similar (presented in **Figure 17**).

Along the Sun's beams, reflection from the snow is a mirror-like reflection. In the opposite direction it is diffuse. The same quality also exists in the case of fresh snow.

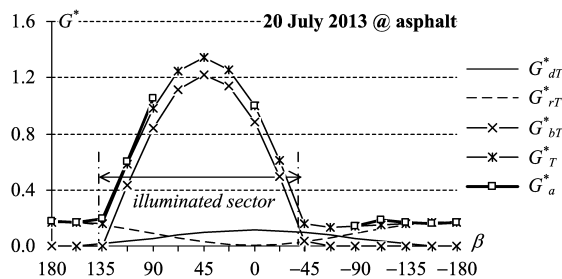


Figure 11. Asphalt surface in sunshine: $G_0 = 607 \text{ Wm}^{-2}$; $\alpha_s = 46.8^\circ$ and $\mathcal{A} = 0.17$.

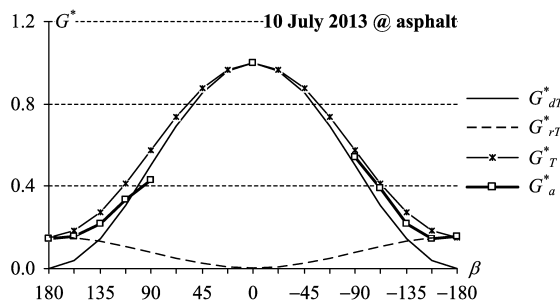


Figure 12. Asphalt surface under an overcast sky (in shadow): $G_0 = 189 \text{ Wm}^{-2}$; $\alpha_s = 49.5^\circ$ and $\mathcal{A} = 0.15$.

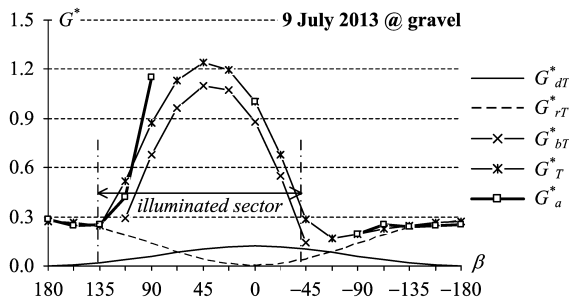


Figure 13. Gravel surface (**Figure 6**) in sunshine: $G_0 = 679 \text{ Wm}^{-2}$; $\alpha_s = 52.5^\circ$ and $\mathcal{A} = 0.19$.

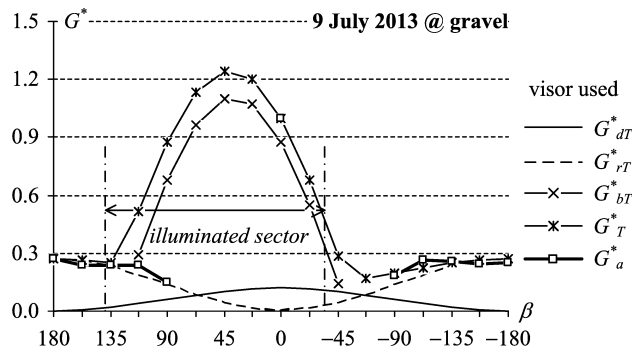


Figure 14. The same gravel surface in sunshine using a visor for $S(90)$: $G_0 = 679 \text{ Wm}^{-2}$; $\alpha_s = 52.5^\circ$ and $\mathcal{A} = 0.19$.

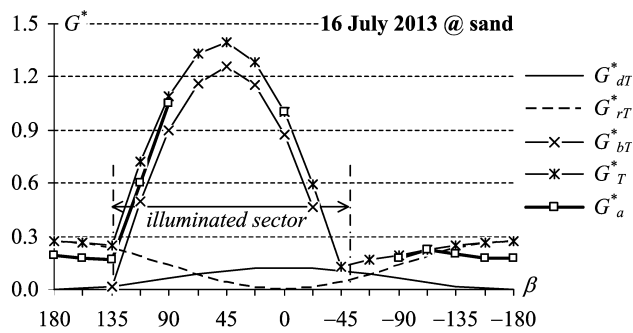


Figure 15. Sandy surface in sunshine: $G_0 = 705 \text{ Wm}^{-2}$; $\alpha_s = 44.5^\circ$ and $\mathcal{A} = 0.19$.

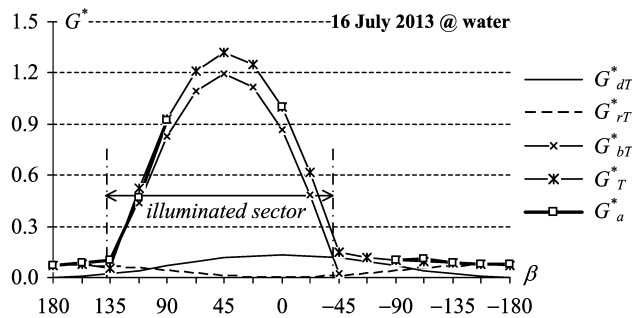


Figure 16. Water in sunshine: $G_0 = 798 \text{ Wm}^{-2}$; $\alpha_s = 46.4^\circ$ and $\mathcal{A} = 0.07$.

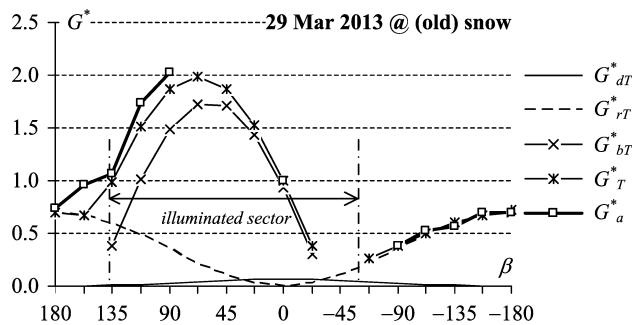


Figure 17. Old snow in sunshine: $G_0 = 585 \text{ Wm}^{-2}$; $\alpha_s = 34.2^\circ$ and $\mathcal{A} = 0.7$.

6. Reliability of the Experiment

Figure 18 shows the stand for the measurements of the reflected radiation at the Toravere Actinometrical Station [10], which is a part of the Baseline Solar Radiation Network (BSRN, [11]) and uses standard equipment. The sensor on the reverse horizontal plane is located away from surrounding objects and supported by a heavy console, the construction of which cannot be realized under portable conditions. Therefore, it may be that the stand used by us includes a systematic error. To prove the lack of such an error, the following test was conducted.

The free carrier ring alone was hung from a cable (at a height of 2 m) over a grass surface (case A) and the irradiance of each sensor was recorded. Then the frame was placed in its position, legs under the ring (case B) and away from the ring (case C) and the recording was repeated.

Figure 19 shows the result of the control: recorded irradiance in relative units based on $S(0)$ of case A proves that the frame (plus operator) does not influence the results (or a possible influence remains within the range of random errors). Therefore, it can be considered that the use of a portable measuring device does not involve systematic errors and the results are reliable.

7. Conclusion

The study proves that the isotropic sky and isotropic ground reflection model warrants calculated values of irradiance in relative units on surfaces inclined due to the ground, which have a good coincidence with their actual values. Usage of the work—measuring current values of the global irradiance on different planes allows the study of the current distribution of irradiance on inclined surfaces (in the real time domain). The said coincidence is



Figure 18. The stand for the measurements of reflected radiation at the Toravere Actinometrical Station (TOR).

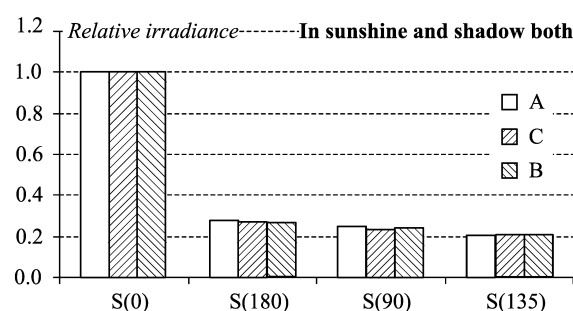


Figure 19. Influence of the frame on the result is lacking.

the best at low albedo, but is not valid for snow-cover due to the Sun. The distribution of irradiance on inclined surfaces with alternating discrete clouds has to be studied specifically.

References

- [1] Thalfeldt, M., Pikas, H., Kurnitski, J. and Voll, H. (2013) Façade Design Principles for Nearly Zero Energy Buildings in a Cold Climate. *Energy and Buildings*, **67**, 309-321. <http://dx.doi.org/10.1016/j.enbuild.2013.08.027>
- [2] Voll, H. and Koiv, T.-A. (2009) Daylight Availability and Cooling in Commercial Buildings—The Influence of Façade Design. *WEAS Transactions on Advances in Engineering Education*, **6**, 316-326.
- [3] Ineichen, P., Guisan, O. and Perez, R. (1990) Ground-Reflected Radiation and Albedo. *Solar Energy*, **44**, 207-214.
- [4] Skartveit, A., Olseth, J.A. and Tuft, M.A. (1998) An Hourly Diffuse Fraction Model with Correction for Variability and Surface Albedo. *Solar Energy*, **63**, 173-183.
- [5] Muneer, T. (2004) *Solar Radiation and Daylight Models*. Elsevier Butterworth-Heinemann, Burlington.
- [6] Tomson, T. (2013) Diffuse Solar Radiation in Estonia. Investigation and Usage of Renewable Energy Sources. *XV Conference Proceedings*, Estonian University of Life Sciences, Tartu, 86-95.
- [7] Liu, B.Y.H. and Jordan, C. (1963) The Long-Term Average Performance of Flat-Plate Solar Energy Collectors: With Design Data for the U.S., Its Outlying Possessions and Canada. *Solar Energy*, **7**, 53-74. [http://dx.doi.org/10.1016/0038-092X\(63\)90006-9](http://dx.doi.org/10.1016/0038-092X(63)90006-9)
- [8] Quashning, V. and Hanitch, R. (1998) Irradiance Calculations on Shaded Surfaces. *Solar Energy*, **62**, 369-375.
- [9] (2014) Soldata Instruments. www.soldata.dk
- [10] Tooming, H. (2003) *Handbook of Estonian Solar Radiation Climate*. EMHI, Tallinn.
- [11] Ohmura, A., Gilgen, H., Hegner, H., Müller, G. and Wild, M. (1998) Baseline Surface Radiation Network (BSR-N/WCRP): New Precision Radiometry for Climate Research. *Bulletin of the American Meteorological Society*, **79**, 2115-2136. [http://dx.doi.org/10.1175/1520-0477\(1998\)079<2115:BSRNBW>2.0.CO;2](http://dx.doi.org/10.1175/1520-0477(1998)079<2115:BSRNBW>2.0.CO;2)

Nomenclature

$\mathcal{A} = G_r/G_0$ —albedo

G , Wm^{-2} —irradiance

G_0 , Wm^{-2} —irradiance on the horizontal plane

G_a , Wm^{-2} —measured actual irradiance on tilted planes

G_b , Wm^{-2} —irradiance of the beam radiation

G_{b0} , Wm^{-2} —beam component of irradiance on the horizontal plane

G_{d0} , Wm^{-2} —diffuse component of irradiance on the horizontal plane

G_{vB} , Wm^{-2} —irradiance on the (shadowed) vertical plane

G_{vF} , Wm^{-2} —irradiance on the (illuminated) vertical plane

G_T , Wm^{-2} —relative irradiance on the on an inclined plane

G_{bT} , Wm^{-2} —beam component of irradiance on an inclined plane

G_{dT} , Wm^{-2} —diffuse component of irradiance on an inclined plane

G_r , Wm^{-2} —reflected irradiance on the reverse horizontal plane

G_{rT} , Wm^{-2} —calculated reflected irradiance on tilted planes

G_{bT} , Wm^{-2} —calculated beam irradiance on tilted planes

G_T , Wm^{-2} —calculated global irradiance on tilted planes

Corresponding relative values are marked with asterisk: $G^* = G/G_0$ —relative irradiance

α_s —height angle of sun

Θ_T —incident angle of the beam radiation

Scientific Research Publishing (SCIRP) is one of the largest Open Access journal publishers. It is currently publishing more than 200 open access, online, peer-reviewed journals covering a wide range of academic disciplines. SCIRP serves the worldwide academic communities and contributes to the progress and application of science with its publication.

Other selected journals from SCIRP are listed as below. Submit your manuscript to us via either submit@scirp.org or [Online Submission Portal](#).

